1-1-2014

Ultra-Wideband Microwave Ablation Applicators

Mustafa Asili

Ultra-wideband microwave ablation applicators

By

Mustafa Asili

A Thesis
Submitted to the Faculty of
Mississippi State University
in Partial Fulfillment of the Requirements
for the Degree of Master of Science
in Electrical and Computer Engineering
in the Department of Electrical and Computer Engineering

Mississippi State, Mississippi

May 2014

Ultra-wideband microwave ablation applicators

By

Mustafa Asili

Approved:

_____

Erdem Topsakal
(Major Professor)

_____

J. Patrick Donohoe
(Committee Member)

_____

Pan Li
(Committee Member)

_____

James E. Fowler
(Graduate Coordinator)

_____

Jason Keith
Interim Dean
Bagley College of Engineering

Name: Mustafa Asili

Date of Degree: May 16, 2014

Institution: Mississippi State University

Major Field: Electrical and Computer Engineering

Major Professor: Dr. Erdem Topsakal

Title of Study: Ultra-wideband microwave ablation applicators

Pages in Study: 45

Candidate for Degree of Master of Science

The increasing demand for efficient cancer treatment inspired the researchers for new investigations about an alternative treatment of cancer. Microwave ablation is the newest ablation technique to cure cancer. This method is minimally noninvasive and inexpensive compared to the other methods. However, current microwave ablation systems suffer due to narrowband nature of the antenna (dipole or slot) placed at the tip of the probe. Therefore, this study developed an ultra-wideband ablation probe that operates from 300MHz to 10 GHz. For this purpose, a small wideband antenna is designed to place at the tip of the probe and fabricated. These probes are tested at ISM frequencies (2.4 GHz and 5.8GHz) in skin mimicking gels and pig liver. Microwave ablation probe design, simulation results, and experiment results are provided in this thesis.

DEDICATION

To my wife, Eda Kara Asili.

ACKNOWLEDGEMENTS

I would like to express my deepest appreciation to my advisor, Dr. Erdem Topsakal for his excellent guidance and patience. I would like to thank Dr. Donohoe and Dr. Li for willing to be my committee members. I would like to thank Erin Colebeck for making gels and getting livers from slaughter house. I would also like to thank my wife and parents for supporting and encouraging me.

TABLE OF CONTENTS

LIST OF TABLES

LIST OF FIGURES

CHAPTER I

INTRODUCTION

Nowadays, there is an increasing demand on noninvasive, inexpensive and harmless ablation techniques that are practical and beneficial. The most known and commonly used one is tumor ablation. Tumor ablation is basically destroying or restoring unhealthy tissue by using heat. If the developments in medicine and science are taken into account, the recent techniques are almost ready to meet the demands of patients who cannot be cured by surgical operations. There are many ablation techniques in terms of cryoablation, direct current catheter ablation (dc shock), laser ablation, ultrasound ablation, radiofrequency (RF) ablation, and microwave (MW) ablation [1], [2], [3]. The purpose of investigating all thermal ablation techniques remains to destroy cancerous cells without harming the healthy ones. The newest tumor ablation modalities are already minimally invasive and painless. The most recent one is MW ablation. It eliminates most of the disadvantages of previous techniques. The first result of MW ablation was published in 1994 [4]. According to Matsukawa et al. in 1997, the response rate of the treatment is 70% for tumors of 3cm or less and 55% for larger tumors [5].

Tumor ablation can also be described as the application of thermal or chemical therapies to tumors to destroy cancerous cells or to achieve substantial tissue destruction. It has been used for more than a century [1], [6]. Thermal ablation modalities are used to treat many tumors of the liver, lung, breast, kidney, bone and pancreas [7], [8]. Thermal

ablations which are minimally invasive and percutaneous can also be used as an adjunctive method for the conventional treatments. Therefore, some incurable diseases like hepatocellular carcinoma (HCC), which is not able to be cured by conventional treatments such as chemotherapy, may be cured by thermal therapy [9]. Ablative therapies are simple, applicable, effective and feasible techniques for untreatable tumors due to the difficulties of surgical resection [8], [10], [11], [12]. Thermal ablation may be a proper treatment for patients who are in the early stage (very small tumor) of cancer and do not want to undergo surgery.

The oldest method used for thermal ablation is cryoablation, also called cryotherapy [13]. It freezes the malignant tissue to destroy by using subzero temperatures [14]. It is still being used today, but its massive nature and complications, such as cryoshock due to freezing tissue, are limiting its worldwide use [15]. Laser ablation is another technique, which uses a thin fiber-optic device to deliver laser energy [16]. Similar to the most other ablation techniques, ineffectiveness of the laser ablation is associated with some problems and limitations, such as penetration inability of light through blood and high cost of equipment, preventing it from becoming more popular.

Ultrasound is one of the modalities used for thermal ablation. It relies upon propagation of a sound wave as a mechanical wave that produces heat in tissue at a frequency range of 2-20 MHz [15]. Although ultrasound ablation provides a coupled system with imaging and ablation systems, producing a durable crystal transducer is a main challenge for this technique.

In 1982, high energy direct current pulse (DC shock) was used for treatment of arrhythmias; however, there are many disadvantages such as pain, requirement of general

anesthesia, and difficulty of controlling the damage. Fortunately, these disadvantages inspired researchers for new investigations for an alternative technique [2], [3]. Nowadays, delivering energy to heat and destroy tissue by using applications of electromagnetic (EM) waves, which does not require a medium to radiate, is becoming more famous, and it is most widely used in United States [19], [20], [21]. Recently, MW ablation, which has many advantages compared to RF ablation, is investigated as a new technique for tumor treatment in different organs.

RF ablation has been used since 1980s due to its ease of use, safety and effectiveness [22]. It is mainly used for many years for ablation of arrhythmias and liver tumors by increasing the temperature of the cancerous tissue around 60 °C [23]. Contact is required between the probe and tumor for recently invented ablation techniques such as laser ablation and RF ablation [9]. The power level of this technique can reach up to 200W in the frequency range of 300 kHz to 1MHz. This procedure relies on the flow of the alternating current of RF waves at very low frequencies through the tissue. In order to make the alternating current flow through the tissue and create a closed circuit, a grounding pad is necessary. RF current creates resistive heating because tissue is not a perfect conductor [24]. Resistive heating is effective only a few millimeters into the tissue, so conductive heating increases the temperature in the rest of ablation zone [25]. When RF power is applied using the probe, RF current is induced between the electrode and the ground pad, which creates frictional heat by changing the direction of ions and generating ionic agitation. This heating causes water loss in surrounding tissues, and cells suffer from coagulation necrosis above 50 °C in a few minutes [10], [15]. The diagram of RF ablation procedure is shown in Figure1.1 [26]. Since the invention of RF ablation, it

has been implemented in dogs [17] and men [18]. It is a minimally invasive, versatile and inexpensive modality when compared to the previous techniques [22]. Beside the advantages of RF ablation, there are several issues associated with the procedure. It depends on the conduction of electric energy into the tissue, so it is limited to the use of single probe. Furthermore, the size of the ablated region in the tissue increases quickly at the beginning of the heating; after temperature exceeds 100 °C, the water content of tissue will vanish, and the rate of increment decays rapidly due to the rise in the impedance and the decay rate of power ($P \sim 1/r^4$), where r is the distance from the probe [3], [27], [28], [29]. Change in impedance with respect to temperature is shown in Figure 1.2 [24]. In addition, pain caused by ablated lesion size and skin burns created by the grounding pad are other major problems of RF ablation [22], [30]. Omnidirectional current flow, which creates undesired ablated zone, between probe and ground pad is another limitation [15]. All these unwanted effects push researchers to find better methods for the treatment of cancerous tumors.

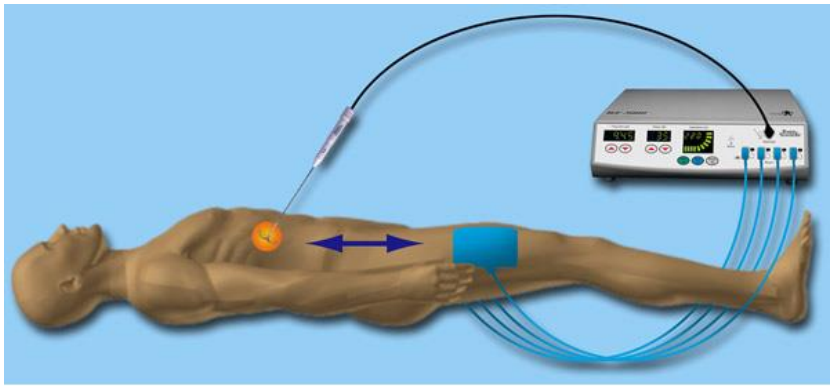

Figure 1.1 Diagram of RF ablation procedure (probe, ground pad and RF generator).

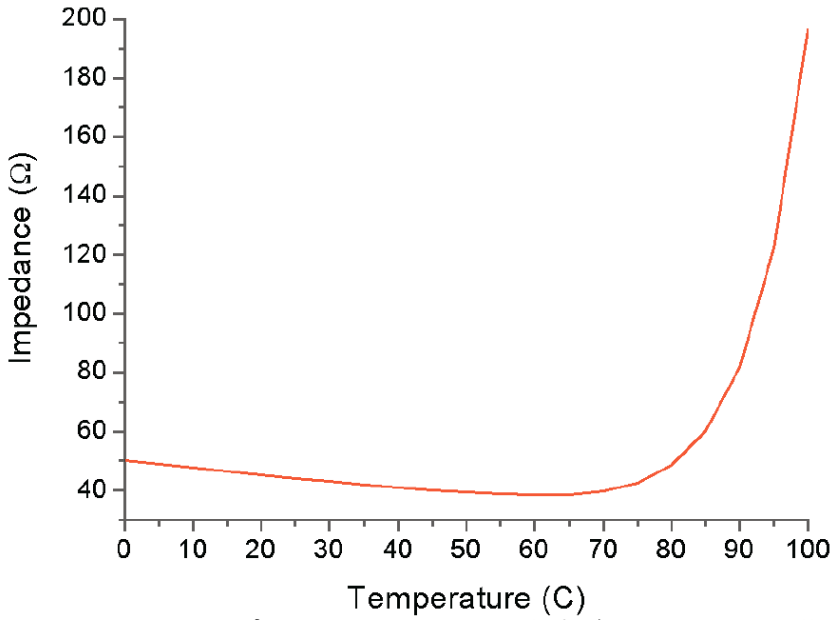

Figure 1.2 Impedance versus temperature during RF ablation.

MW ablation is the newest modality used for tumor ablation similar to RF ablation [15]. The first open surgical MW ablation was in Japan in 1990s at 2.45 GHz [4], but the first operation in the US was performed in 2003 at 915 MHz [31]. The most commonly used frequency range allowed by Federal Communications Commission (FCC) for MW ablation is from 915 MHz to 2.45 GHz. MWs can focus the energy directly into the tissue with the help of shorter wavelengths compared to RF ablation [15], and MW ablation does not rely on conduction of the alternating electrical current, so it causes less pain. It bases on the propagation of EM wave that increases the temperature of tissue fast and homogeneously [32]. Required equipment includes a MW ablation catheter (MW antenna), a MW generator, and a thermometry or imaging system to monitor the temperature changes. The current MW ablation system setup is shown in Figure 1.3 [1].

a. b.

Figure 1.3 MW ablation system setup: a) applicators, b) applicators and generators.

To apply this method, a microwave antenna (applicator) is placed directly into the target zone, and EM waves coming from MW generator propagate through the applicator. The system does not require a ground pad because of the nature of MW. MWs produce friction and heat by waving water molecules in the surrounding tissue [1]. This heat and friction causes cell death and creates an ablation zone [1]. Unlike RF ablation, MW ablation offers multi-probe application simultaneously. An operation of liver tumor ablation with MW multi-probes from University of California is shown in Figure 1.4 [33].

Figure 1.4 Liver tumor ablation at University of California, San Diego in 2009.

In physics, polar water molecules (H_2O), which have positive and negative charges, oscillate and flip due to the electric charge in EM radiation. This continuous oscillation of positive and negative charges in accordance with MW frequency results in kinetic energy and heat generation; heat created by movement of dipoles (water molecules) causes cell death [1]. The effect of microwaves on water molecules is shown in Figure 1.5 [1].

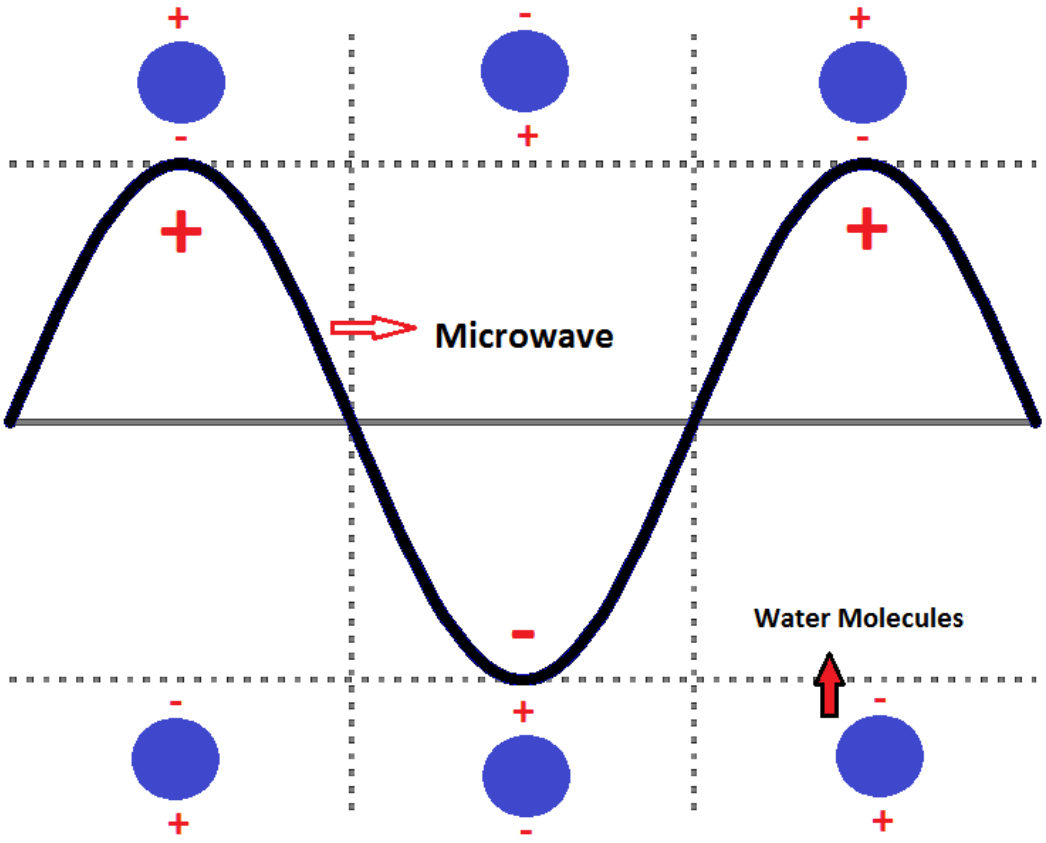

Figure 1.5 Interaction between water molecules and microwave.

MW ablation provides many advantages in addition to the benefits of RF ablation with potential to eliminate the problems associated with RF ablation [34], [35]. In contrast to RF ablation, MW ablation eliminates potential unwanted skin burns caused by the ground pad. As it is reported in literature, MW ablation can provide much deeper ablation zone because of slower decay of power deposition at higher temperature as shown in Figure 1.6 [24], and faster heating [15], [36], [37]. In Figure 1.6 provides a comparison of temperature increase during RF ablation with 200W input power and MW ablation with 60W input power at 2.45 GHz. Temperatures are monitored 5mm from the applicator while heating the tissue. It suggests that after a certain time, RF ablation cannot be performed anymore. During RF ablation, tissue temperature needs to be controlled to prevent from charring and increased impedance; however, MW ablation provides rapid heating in shorter time without considering the impedance [32]. Also, lesion volume can be larger by increasing the power and duration [38]. For RF heating, electrical conductivity is important as a tissue property, while MW can propagate through tissue even with zero conductivity [24]. MW ablation is dielectric heating, so relative permittivity (ε_r), which is a measure of the resistance of a material to formation of electric field, is important as a tissue property [24].

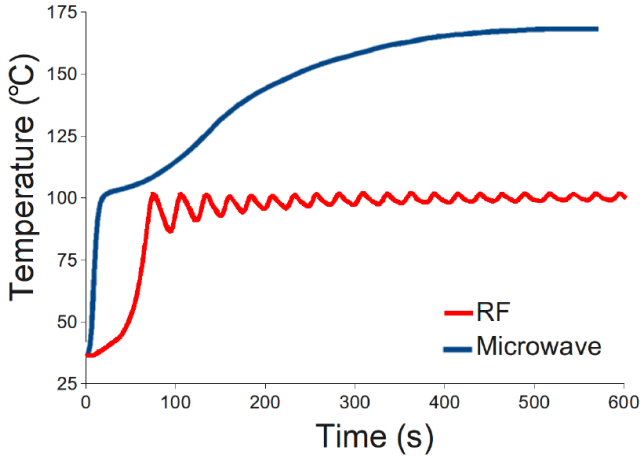

Figure 1.6 Comparison of increase in temperature during MW ablation (60W) and RF ablation (200W).

Despite many advantages, there are still major problems associated with the current MW ablation systems. In MW ablation, the most important and the most critical elements are MW antennas. Impedance matching is one of the main challenges. If antenna impedance is not matched to the feed line, usually coaxial lines, power dissipation and return loss referring reflection of the most of applied power from the antenna increases. During ablation procedure, the properties of tissue that affect the resonation of the antenna changes because of heating and evaporation. Resonation frequency of antenna may shift to another frequency range after a few seconds. Applicators of current MW ablation systems are designed for only one frequency (e.g. 915 MHz or 2.45 GHz), and problems are mainly due to the narrowband nature of the antennas used in these systems; thus more than one applicator may be required depending on the size of the target zone during the application. Nevertheless, this issue can be overcome by making the bandwidth of the antenna wider. In order to eliminate these problems, we propose to utilize ultra-wideband antennas for more efficient and unique

MW ablation therapy. In this study, an antenna (applicator) design for MW ablation, tests of antenna in liver, and results are proposed. We have developed very small-sized (5.5mm x 5.5mm) ultra-wideband antennas that can be utilized for MW ablation of liver. We have designed the antenna by using finite element method (FEM) solver, HFSS, considering dielectric properties of tissue. We provide theory behind the antenna design, and present return loss results. In addition, we have shown the effects of changes in temperature on return loss and point of antenna resonation. Finally, we validate the proposed technology using ex vivo pig liver experiments.

CHAPTER II

ANTENNA DESIGN BASICS AND MICROWAVE ABLATION PROBES

2.1 **Antenna Design Basics**

In this thesis, ultra-wideband probes are designed for ablation therapies. Microwave antennas are placed at tip of the probes. Some antenna basics are applied in the design step of the probe used for this application. Firstly, we can start with the definition of antenna. An antenna can be described as a device that converts electromagnetic signals in the electrical currents. It can be used as a transmitter or receiver. The IEEE definition for antenna is: "The part of a transmitting or receiving system that is designed to radiate or receive electromagnetic waves" [39].

There are some basic principles for all types of antennas. Radiation is one of them, and it can be generated by acceleration of charge or time-varying current for an antenna. Radiation cannot occur without accelerating or decelerating motion of charge in a wire. It can be mathematically expressed as in the following equation.

$$i.l = Q.a \tag{2.1}$$

i represents time changing current ($A.s^{-1}$), l is the length (m), Q is charge (C), and a is charge acceleration ($m.s^{-2}$).

Functionality of an antenna is measured by some important parameters which affect the antenna's performance. Some of them are described in the rest of the chapter.

The fields around the antenna can be divided into three zones; one is reactive near field region, one is radiating near field region that can be also called Fresnel region, and other one is far field (Fraunhofer) region [40]. The boundaries of each region are expressed in the following equations [29]. These regions around the antenna are demonstrated as in Figure 2.1.

$$R_1 < 0.62\sqrt{\frac{D^3}{\lambda}} \tag{2.2}$$

$$0.62\sqrt{\frac{D^3}{\lambda}} < R_2 < 2\frac{D^2}{\lambda} \tag{2.3}$$

$$R_3 > 2\frac{D^2}{\lambda} \tag{2.4}$$

R_i (i=1, 2, or 3) is the radius of each circle shown in Figure 2.1 (m), D is the largest dimension of the antenna (m), and λ is wavelength (m). The effect of the ablation probe on the liver in near field region at 2.45 GHz is also demonstrated in Figure 2.1[34]. In Figure 2.1, a half wave dipole antenna is considered as an applicator, and calculations of R_1 and R_2 are depending on the dimensions of a half wave dipole at 2.45 GHz (R_1= 2.68cm, R_2=4.82cm).

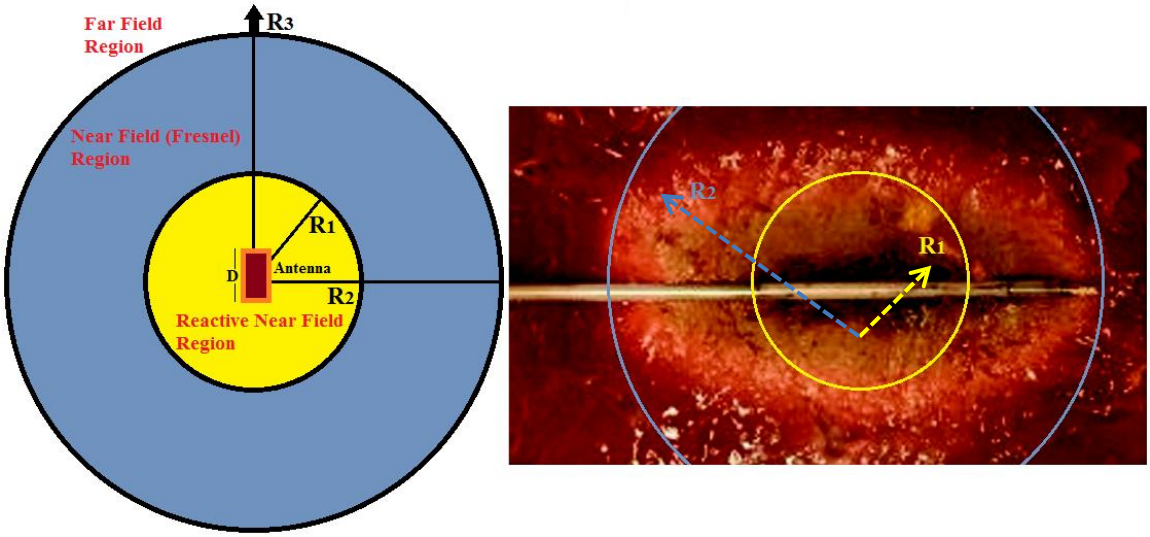

Figure 2.1 Fields around an antenna (reactive and radiating regions) and effect of ablation at 2.45 GHz.

In reactive near field region, since reactive fields take place, there is no energy dissipation [41]. In Fresnel region, radiating fields are dominating compared to reactive near field region. In far field region, there is no reactive field. Electric and magnetic fields attenuate with $1/R^3$ and$1/R^2$ in reactive near field region and Fresnel region, respectively while fields die off with 1/R in far field region. On the other hand, this is another disadvantage of designing an antenna for ablation. Radiation cannot last long in near field, so EM wave cannot penetrate more than a few centimeters, which means ablation zone is limited. Electric and magnetic fields are also out of phase in reactive near field region while radiating fields are in phase. Increasing medium density compared to air also limits the penetration. As seen in the equations below, a rise in relative permittivity of the medium causes decreasing in the speed of light and wavelength. Decrease in the wavelength results in expending of near filed region.

$$\mu_0 \varepsilon_0 = {}^{1}/_{c^2} \tag{2.5}$$

$$\mu \varepsilon = {}^{1}/_{v^2} \tag{2.6}$$

$$\mu = \mu_0 \mu_r \, , \; \varepsilon = \varepsilon_0 \varepsilon_r \tag{2.7}$$

$$\lambda = {}^{c}/_{f} \;\; or \;\; \lambda = {}^{v}/_{f} \tag{2.8}$$

μ_0 is vacuum permeability, ε_0 vacuum permittivity, μ_r is relative permeability, ε_r relative permittivity, c is the speed of light in vacuum, v is the speed of light in medium, λ is wavelength, and f is the operating frequency of the antenna.

Reflection coefficient (Γ) is another important parameter for antenna functionality. In a transmission line, the reflection coefficient shows how much power is reflected from the load. Generally, implanted antennas and ablation probes are fed by coaxial cable and, if the Figure 2.2 and the equation are considered, effects on the power transmission can be extrapolated.

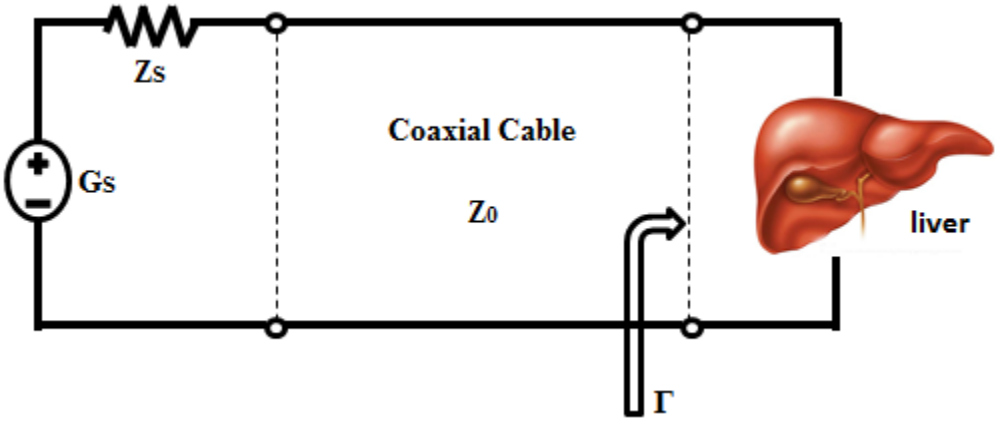

Figure 2.2 Reflection coefficient in a transmission line.

G_S is the source, and Z_S is source impedance. Z_0 and Z_L represent the characteristic impedance of coaxial cable and load (liver) impedance, respectively. As seen in the equation below, any changes in the load affects the reflection coefficient, hence power transmission efficiency is affected.

$$\Gamma = \frac{E^-}{E^+} = \frac{Z_L - Z_0}{Z_L + Z_0} \tag{2.9}$$

If the antenna is not matched perfectly to the coaxial cable or feed line, it will cause undesired tail heating. Figure 2.3 [34] shows a sample view from an application of MW ablation resulted in undesired ablation zone because of antenna mismatch.

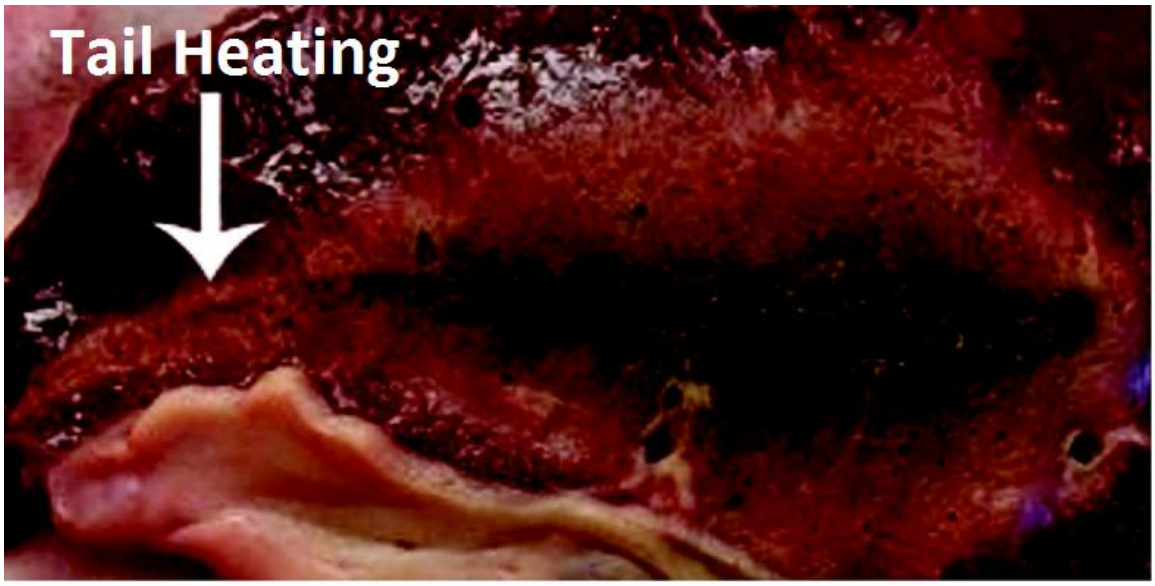

Figure 2.3 Tail heating caused by mismatch.

In practice, S_{11} is the most important parameter in a single-port system. It is a function of reflection coefficient as described in the following equation.

$$S_{11} = 20 \log \Gamma \tag{2.10}$$

Bandwidth is the frequency range in which an antenna can operate efficiently. The bandwidth of broad band antennas and narrow band antennas are different from each other. For a broad band antenna, bandwidth is the ratio of the upper frequency to lower frequency of desired range. For a narrow band antenna, it is defined as the percentage of the upper and lower frequency difference over the center frequency [42]. Mathematical expressions of both broad band and narrow band are shown in the equation (2.11) and equation (2.12), respectively. Simple representation of bandwidth is shown in Figure2.4.

$$BW_b = \frac{f_H}{f_L} \tag{2.11}$$

$$BW_n = \left[\frac{f_H - f_L}{f_C}\right] 100 \tag{2.12}$$

f_H is upper frequency, f_L is lower frequency, and f_C is the center frequency. An antenna can be classified as broad band if upper frequency is at least two times larger than lower frequency.

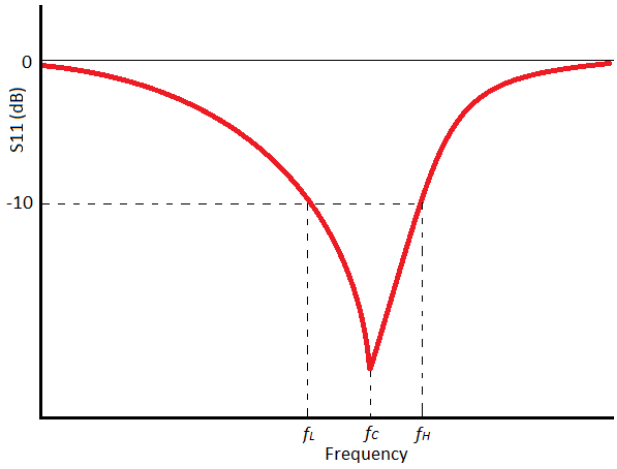

Figure 2.4 S_{11} with upper, lower and center frequencies.

Current ablation systems have narrow band antennas such as dipole and slot antennas. Figure 2.5 shows the bandwidth of current ablation probes, and Figure 2.6 shows the bandwidth of the designed probe in this study.

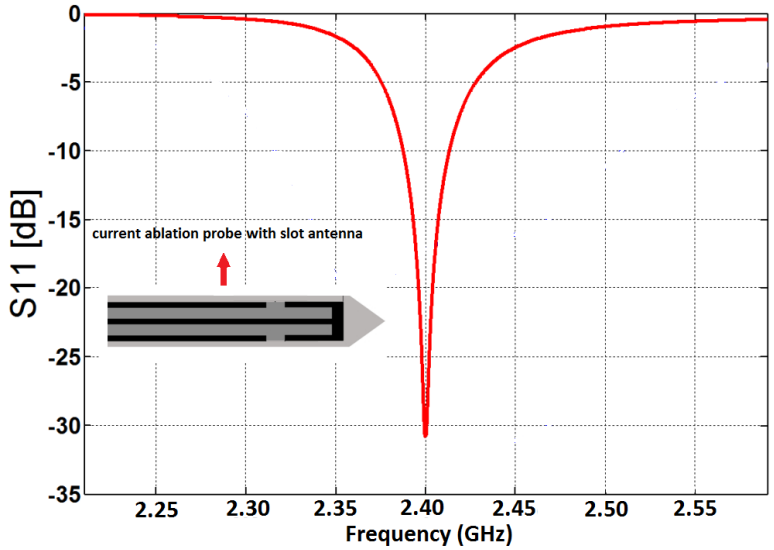

Figure 2.5 S_{11} (return loss) of the current ablation probes with slot antenna.

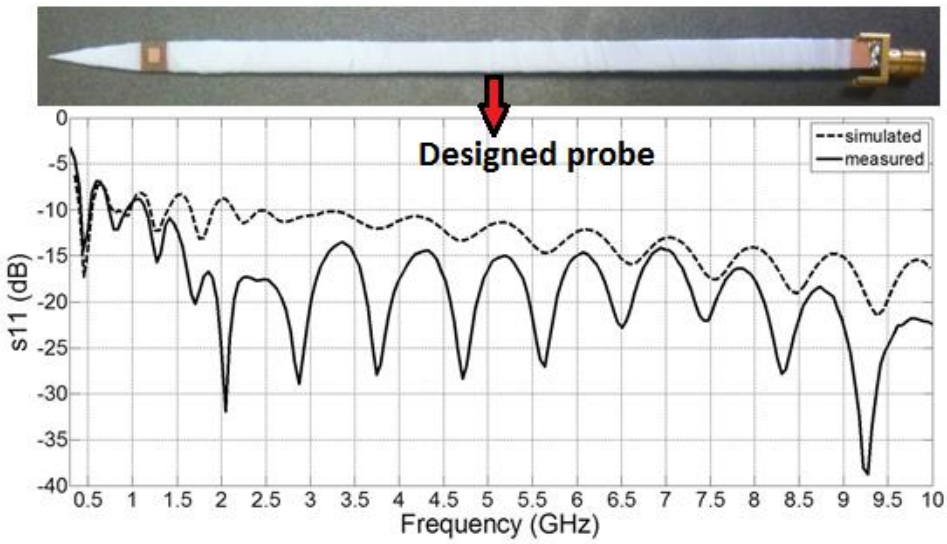

Figure 2.6 S_{11} of the designed microwave ablation probe.

2.2 Microwave Ablation Probe Design

The purpose of this study is to design an ultra-wideband antenna to be used as a MW ablation probe. As mentioned above, the current MW ablation systems suffer due to narrow band nature of the antenna placed at the tip of the probe. An illustrative example will be presented to show how narrow band antennas can degrade the power transmission efficiency. Consider the dipole antenna in Figure 2.7 (designed for ablation at 2.4 GHz). It has been embedded into a medium emulating the electrical properties (dielectric constant - ε_r and conductivity - σ) of the liver tissue. It is a known fact that temperature changes affect the electrical properties of the tissue. Decrease in dielectric constant and conductivity is indicated in Figure 2.8 and Figure 2.9, respectively.

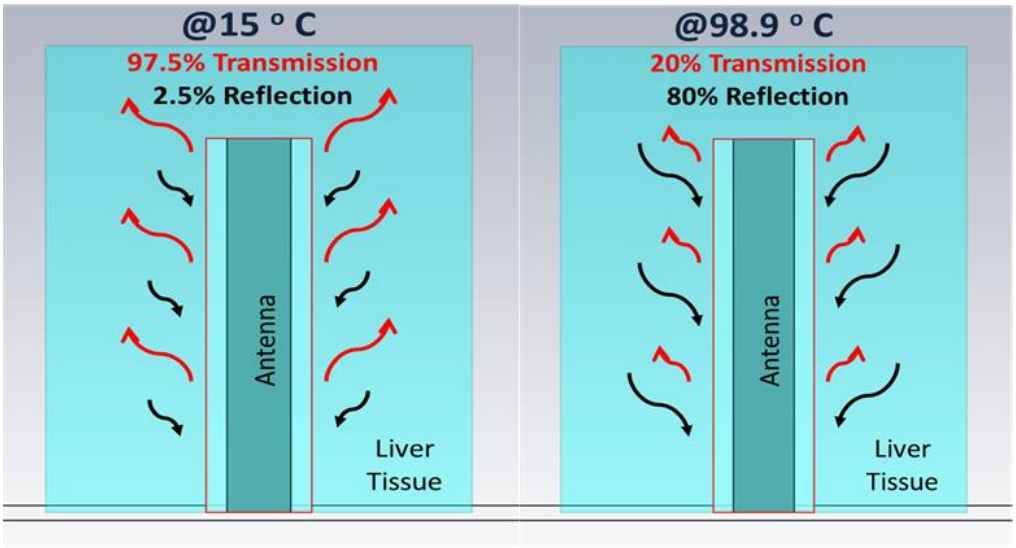

Figure 2.7 Dipole antenna matched the surrounding liver tissue electrical properties at 15 °C providing 97.5% power transmission as opposed to 20% power transmission when temperature is at 98.9 °C.

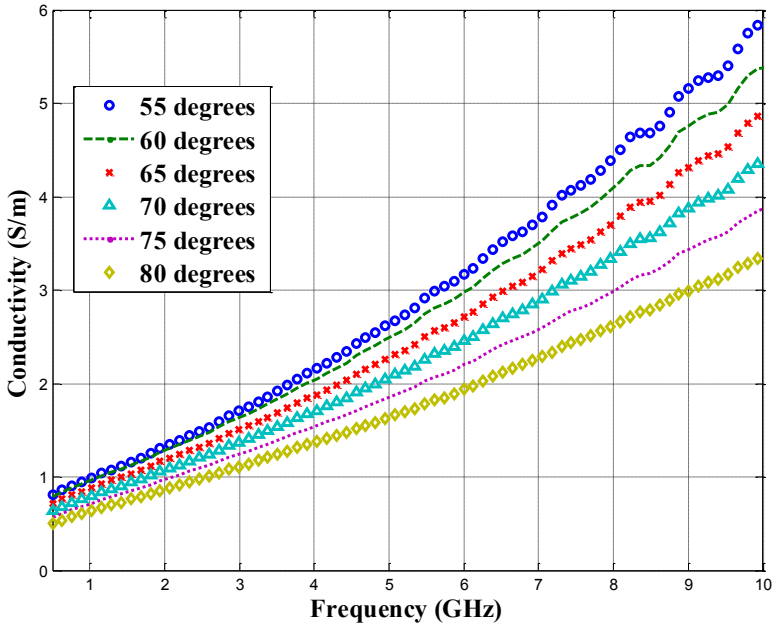

Figure 2.8 Effect of heating on conductivity of pig liver.

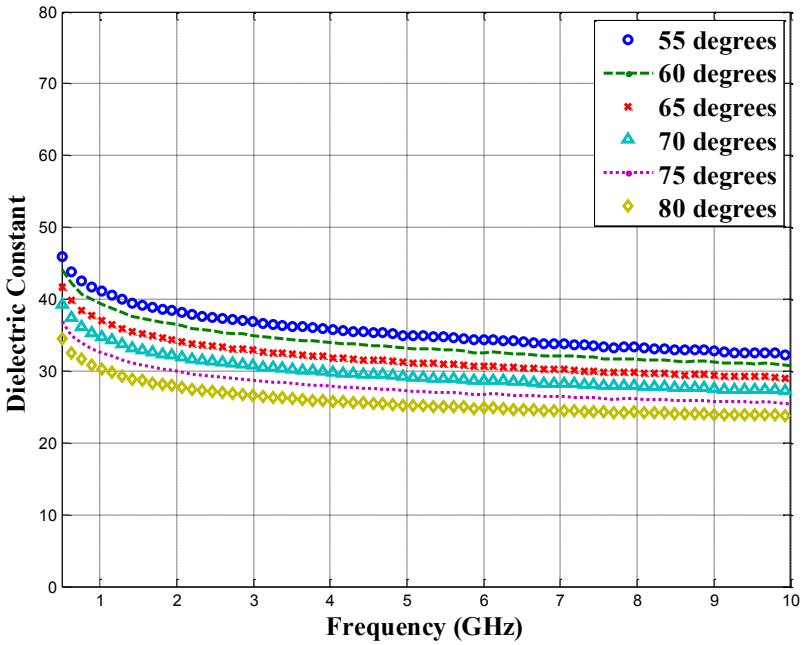

Figure 2.9 Effect of heating on relative permittivity of pig liver.

In addition, the tissue loses water content during heating process because of the generation of water vapor and the diffusion of liquid [36]. As a result, ε_r (from 44.98 to 26.76) and σ (from 1.79 to 1.26) significantly drop as the tissue temperature increases from 15 ^oC to 98.9 ^oC, which is shown in Figure 2.11, because these properties are directly related to water content of the tissue. These changes deteriorate the matching of the antenna impedance to the surrounding tissue impedance, resulting significant drop in power transmission efficiency. As it is mentioned above, the change in load impedance causes mismatch, so power reflection will be increased. And here, antenna in pig liver is considered as load. The red curve in Figure 2.10 is the reflection curve at the start of the ablation procedure. The arrow on the red curve shows the minimum reflection point at 2.4 GHz with 2.5% reflection and 97.5% power transmission into the liver. However, as the temperature increases, the red curve approaches the blue curve, shifting the minimum reflection point further away from 2.4 GHz. At the end of the ablation procedure (at 98.9 ^oC), the arrow on the blue curve indicates that only 20% of the power is transmitted efficiently into the tissue while 80% is reflected back to the probe. This inefficient power transmission into the tissue results in unwanted ablation regions, higher input power requirements, and longer ablation times.

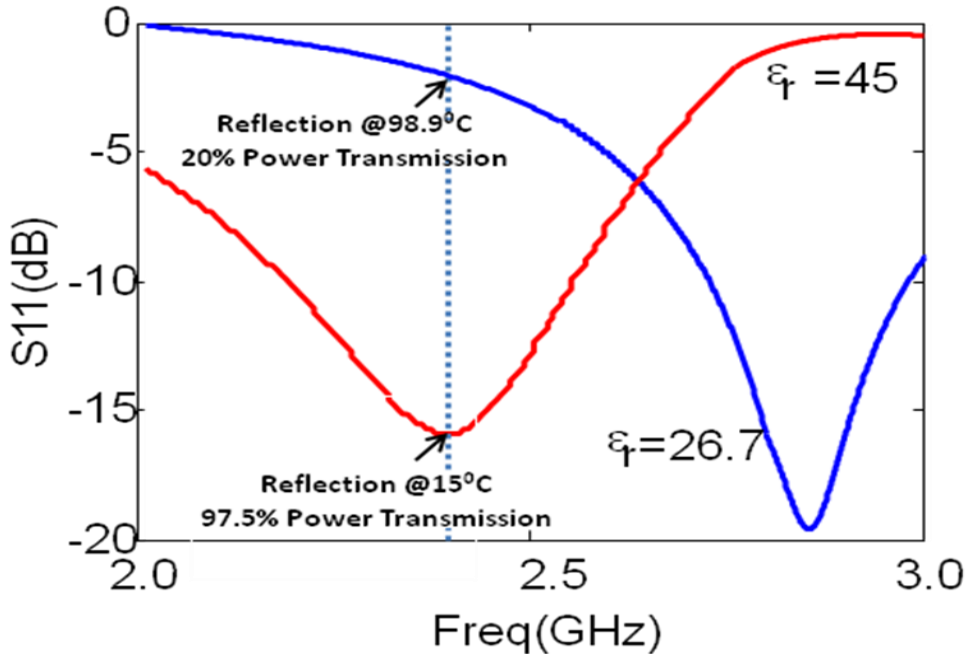

Figure 2.10 The dip on the red curve in the plot shows the frequency of operation at 2.4 GHz before the ablation procedure begins.

A slot between two different media behaves like a leaky wave antenna. For a small width of the slot w_s, (compared to the media on either side of the slot) between two different dielectric media, the asymptotic value of the complex propagation constant is given by Equation (2.13) where γ_e is the Euler's constant, i is positive integer, and k_o is the free space propagation constant.

$$k_w = \frac{}{2\left[1-\frac{4}{\pi}\ln\left(\quad .\quad \frac{}{8}\right)\right]} \tag{2.13}$$

$$k_d = \sqrt{\quad -} \tag{2.14}$$

$$\beta = \sqrt{(\quad - \quad)/2} \tag{2.15}$$

$$k_i = \sqrt{\quad} \tag{2.16}$$

The rays are launched in the dielectric with lower dielectric constant with an angle γ with respect to the slot axis given by Equation (2.17).

$$\frac{}{\varepsilon_{r1}+\varepsilon_{r2}} \tag{2.17}$$

The above equation indicates that the direction of the main beam is essentially independent of frequency, and we have utilized this phenomenon to design extremely small antennas that can be used for in-body applications. For this, it has been exploited that the high dielectric constant of human tissues and low permittivity and low loss material like the FR4 epoxy on which the antenna is printed. The geometry of the antenna used for ablation is shown in Figure 2.11.

The antenna on the probe is designed in the length of quarter-wavelength antenna; then it is coiled to make it much smaller.

$$\lambda = \frac{C}{f} \tag{2.18}$$

$$L = \frac{1}{4}\lambda \tag{2.19}$$

λ is wavelength (m), C is speed of light ($3\text{x}10^8$ m/s), f is frequency and L is the length of antenna. The dimensions of the probe are provided in Table 2.1

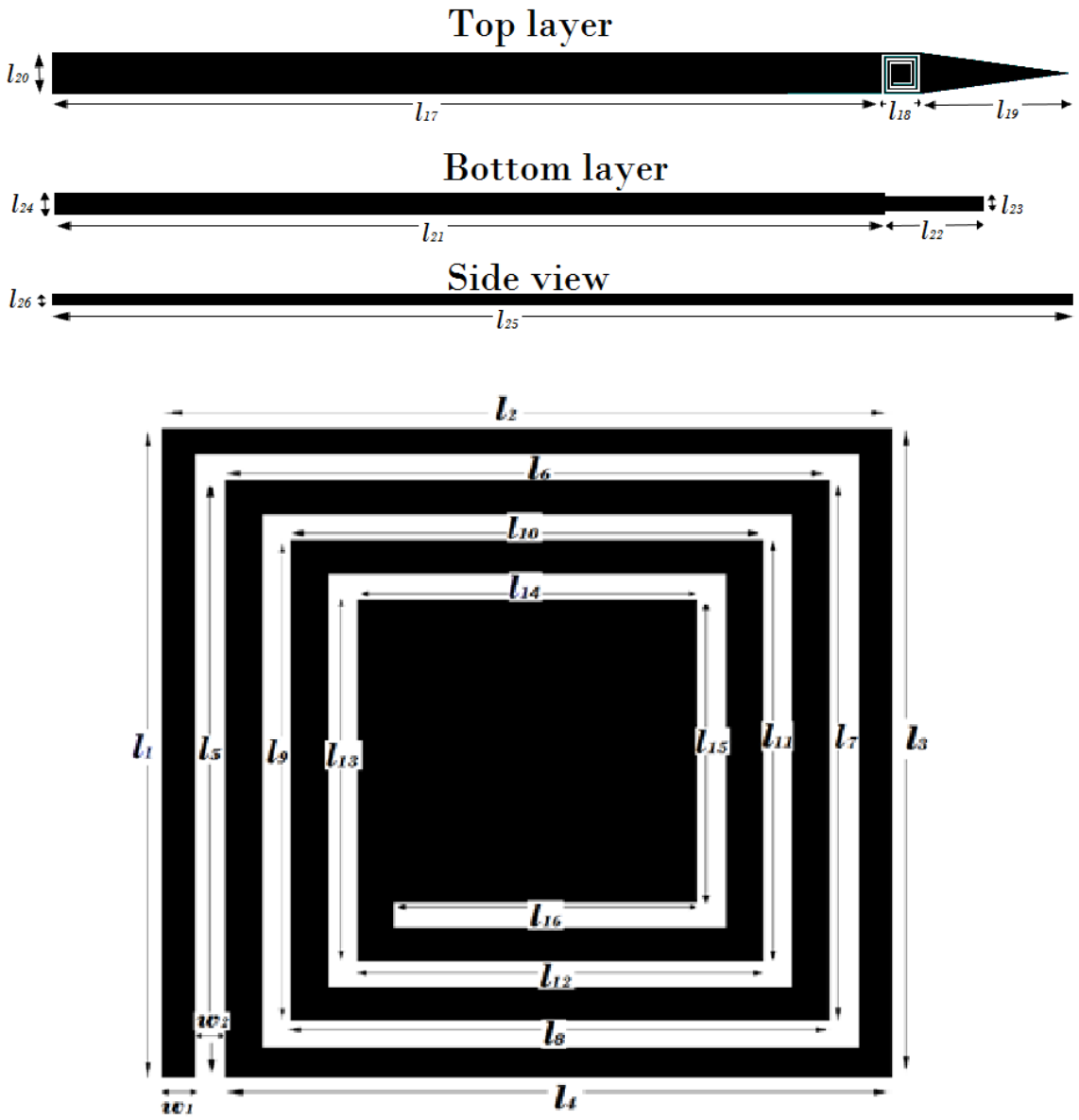

Figure 2.11 Ablation probe used in liver test and antenna on top of the probe.

Table 2.1 Dimensions of MW ablation probe

Symbol	Dim.(mm)	Symbol	Dim.(mm)
l_1	5,5	l_{15}	2,5
l_2	5,5	l_{16}	2,25
l_3	5,5	l_{17}	150,25
l_4	5	l_{18}	5,25
l_5	5	l_{19}	20
l_6	4,5	l_{20}	5,5
l_7	4,5	l_{21}	150
l_8	4	l_{22}	15,5
l_9	4	l_{23}	2
l_{10}	3,5	l_{24}	3
l_{11}	3,5	l_{25}	157,5
l_{12}	3	l_{26}	1,5
l_{13}	3	w_1	0,25
l_{14}	2,5	w_2	0,25

It consists of slot which is coiled in a small area (5.5 mm x 5.5 mm) printed on FR4 ($\varepsilon_r = 4$) substrate and micro-strip line printed on the back side which provides the excitation (Figure 2.12).

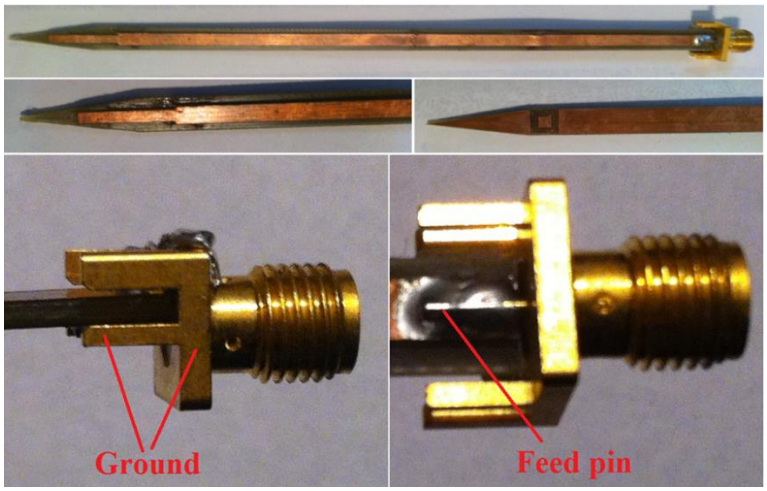

Figure 2.12 Micro-strip line at the bottom of the applicator and SMA connector.

The antenna is provided with a tapered tip FR4 substrate for easy insertion into the tissue. Edge-mount SMA connectors that do not require drilling the substrate are used for connection between amplifier and applicator. The slot, when excited with a suitable micro-strip excitation that couples electromagnetic waves through the slot above, generates leaky waves over a very large bandwidth. The measured and simulated bandwidth of the fabricated MW ablation antenna in skin mimicking gel will be provided in Chapter III (Figure 3.1).

Specific absorption rate (SAR) results and antenna design with different views, including the probe encased in a skin mimicking medium from HFSS, are shown in Figure 2.13, Figure 2.14 and Figure 2.15, respectively. SAR results are provided for 2.4 GHz and 5.8 GHz. These frequencies are ISM frequencies (Industrial, Scientific, and Medical) that are regulated by FCC. The difference between the absorption characteristics for 2.4 GHZ and 5.8 GHz can be clearly seen in Figure 2.13, 2.14, and 2.15. Figure 2.16 is provided to show the gain pattern of the MW antenna. Moreover,

Figure 2.17 shows the effect of temperature rise on SAR values. As shown in the figure, SAR values show a slight increase in SAR with decrease in conductivity, which means there will be more absorption of electromagnetic radiations in tissue with lower conductivity.

Ansys HFSS provided by Ansoft is used as the FEM solver to create and simulate the probe design. During the design, skin is considered as the dielectric medium. Dielectric properties of the skin embedded in HFSS are taken from reference [43]. In tests, the fabricated probe is first tested in skin mimicking gels. Skin mimicking gel is developed in the laboratory by combining de-ionized water, diethylene glycol butyl ethen (DCBE), polyethylene glycol mono phenyl ether (Triton X-114), and salt [44], [45].

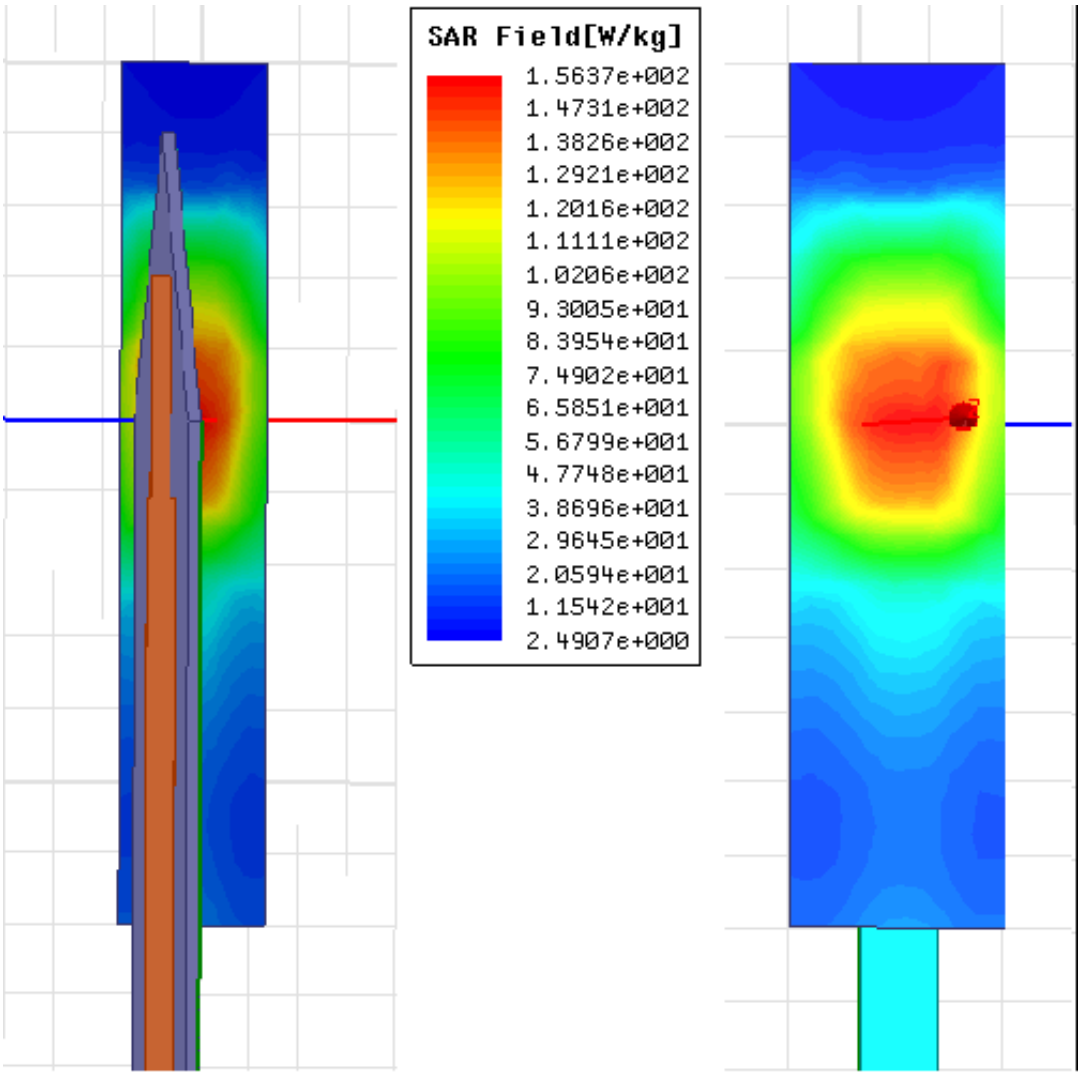

Figure 2.13 Specific Absorption Rate (SAR) at 2.4 GHz

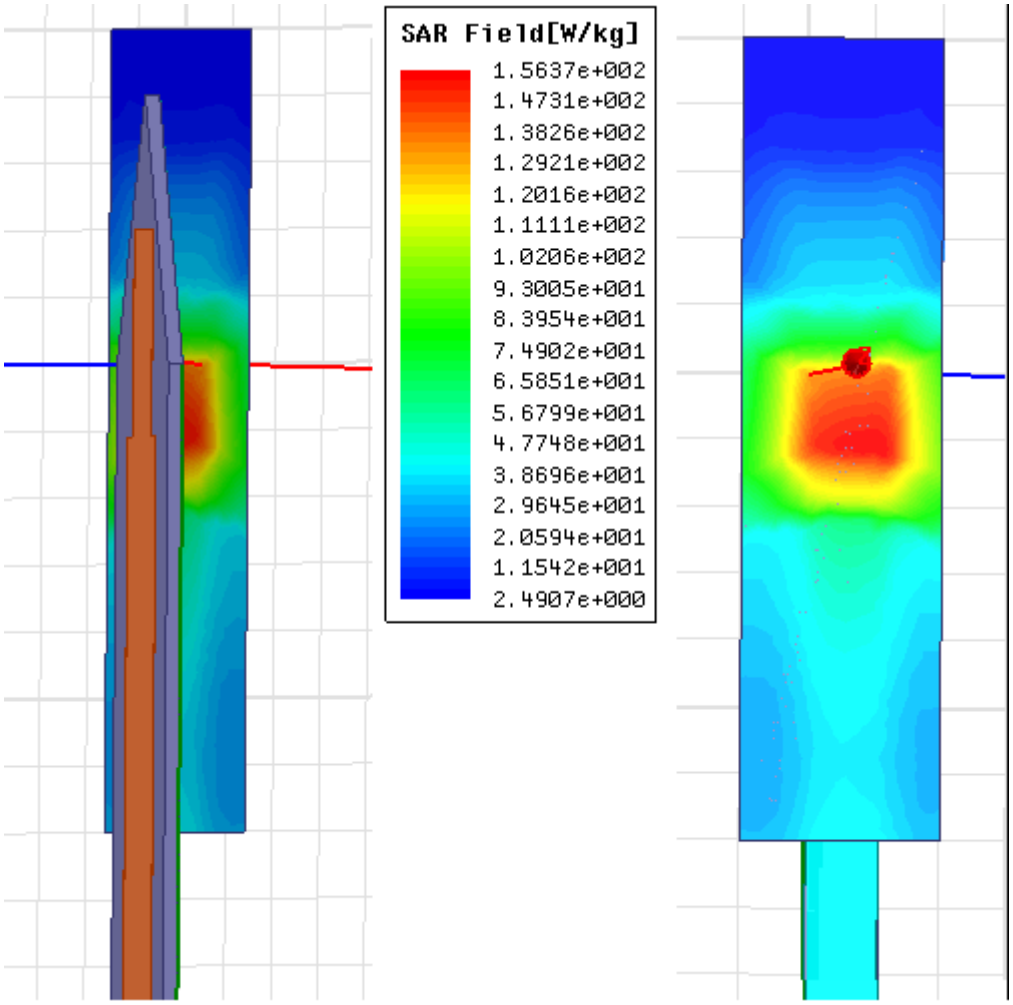

Figure 2.14 Specific Absorption Rate (SAR) at 5.8 GHz.

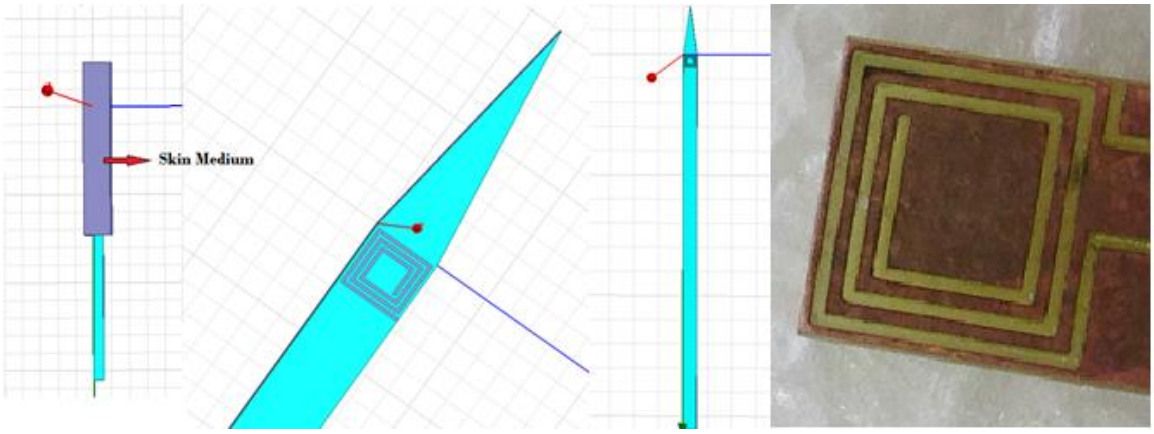

Figure 2.15 Antenna view in HFSS.

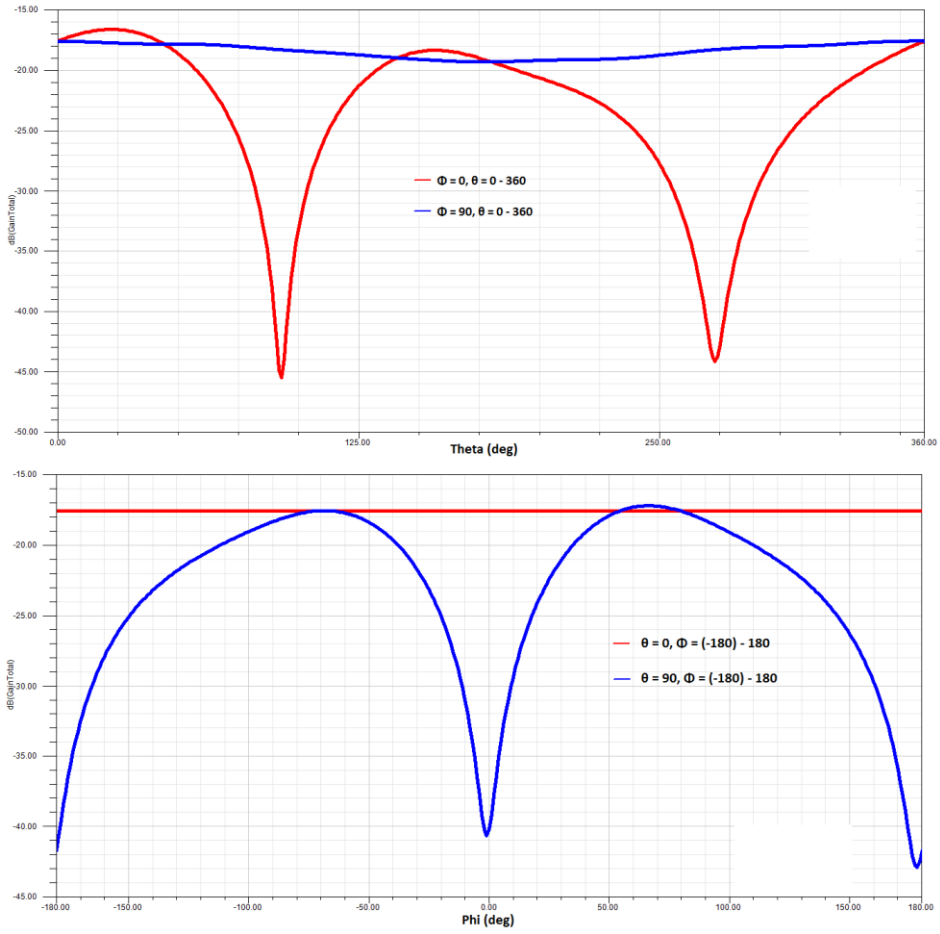

Figure 2.16 Gain patterns.

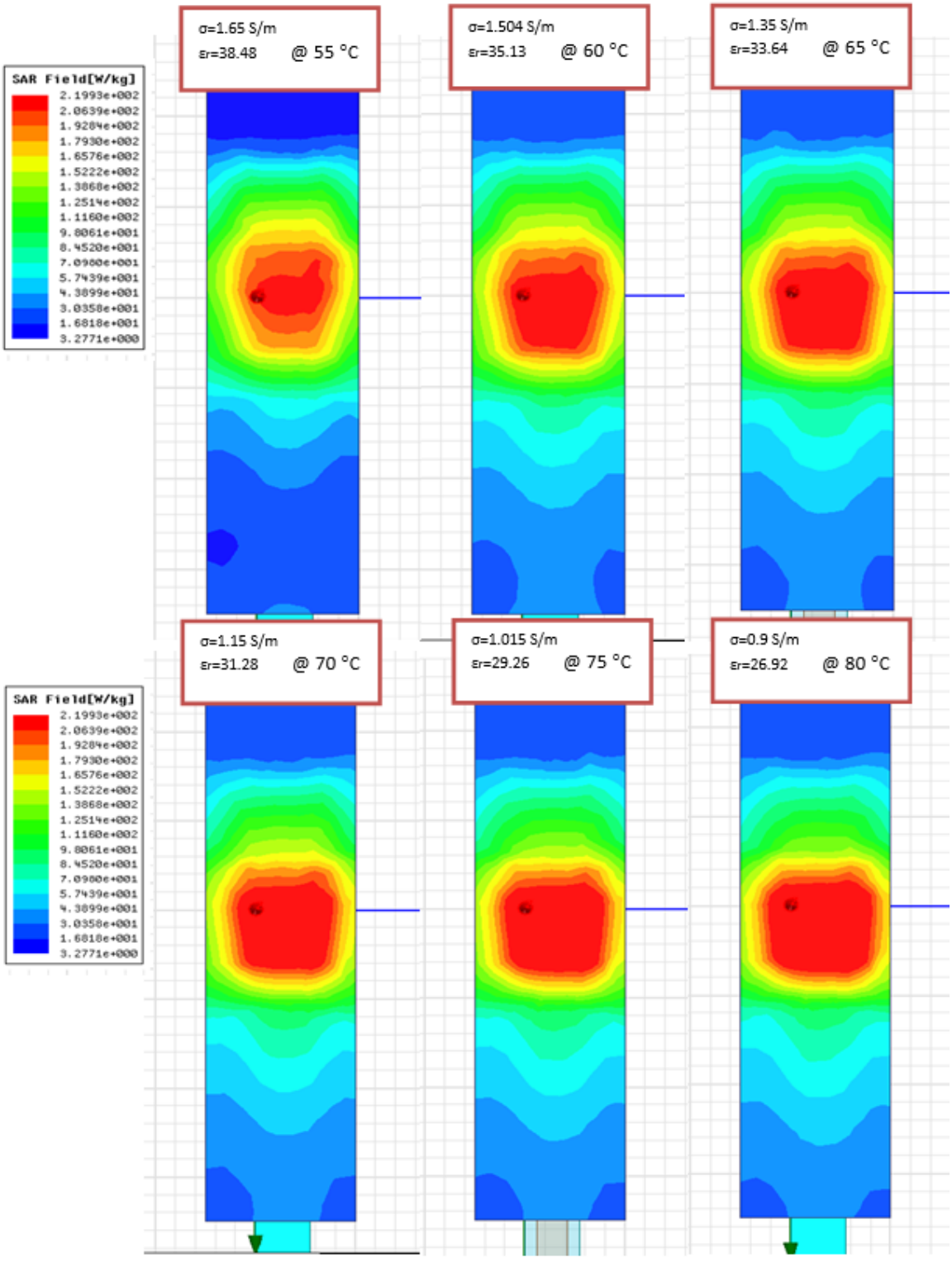

Figure 2.17 Change in SAR values with increase in temperature.

2.3 **Ablation Probe Fabrication**

After the finalization of the design and simulations, I proceeded with the fabrication of the probe. For the first step of the fabrication, required files (.DXF files) are exported from HFSS to be used by in our milling machine. The second step is to process these files. This is done by the transition software called Circuit CAM 6.1 on a computer that controls the milling machine. After the files are exported for the control software BoardMaster 5.1.210 of milling machine, probes were ready to be fabricated. ProtoMat S62 milling machine from LPKF was used to fabricate the antennas. Three probes were fabricated and tested using pig livers. Following the fabrication, probes are isolated with teflon tape to block radiation and undesired ablation zone due to feeding line, and only the tip of the probes (antenna) are left uncovered as seen in Figure 2.18.

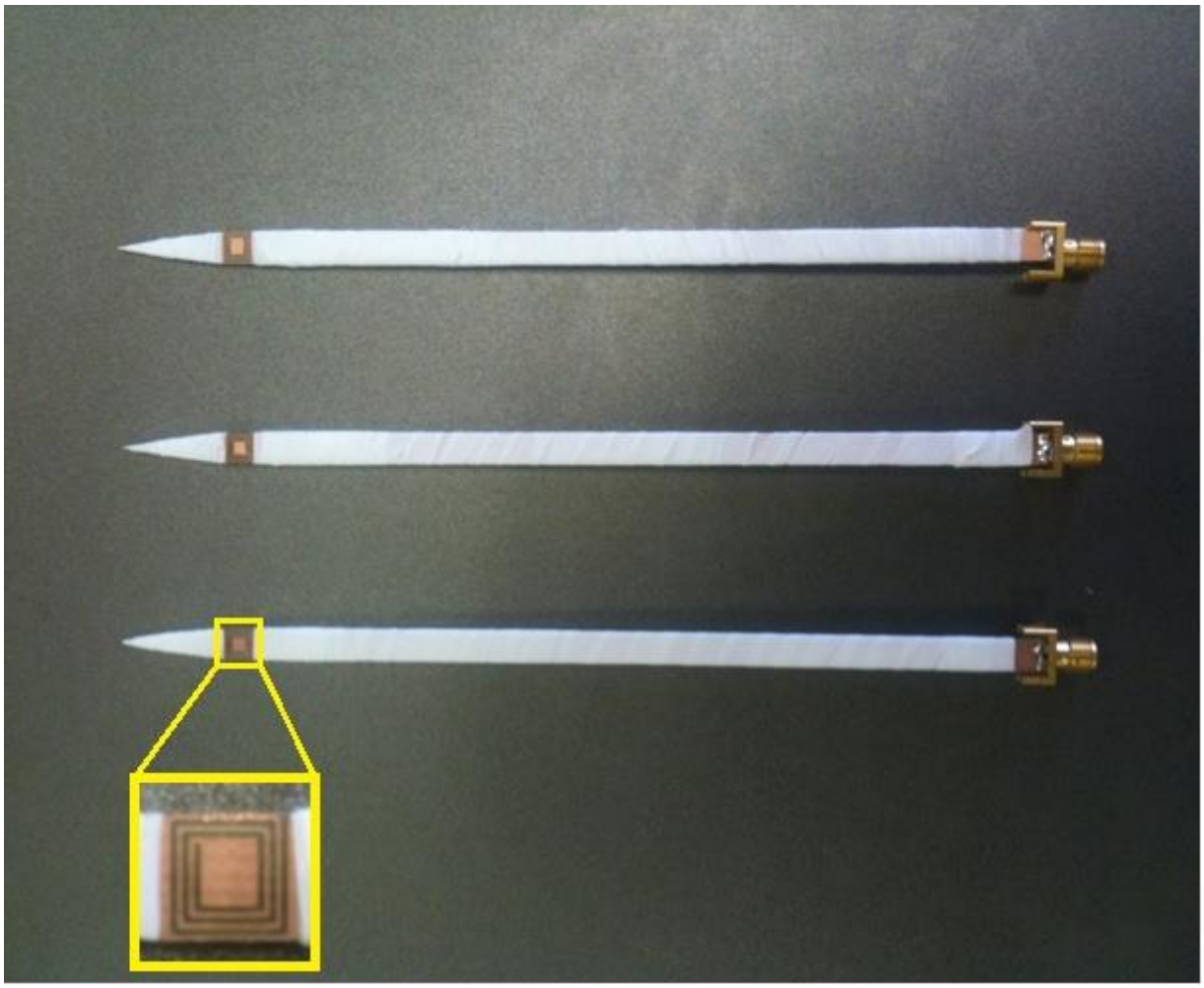

Figure 2.18 Fabricated MW ablation probed covered with teflon tape.

CHAPTER III

IN VITRO TESTING IN GELS AND EX VIVO TESTING IN ANIMALS

In this study, 2.4 GHz and 5.8 GHz are the two main frequencies used for measurements. These frequencies are used in both in vitro and ex vivo measurements. In vitro measurement is performed in skin mimicking gels because, during the initial design of the probes, skin is considered as high dielectric medium in HFSS. Dielectric properties of both skin and liver are close to each other. Therefore, these tests give reliable data before ex vivo animal measurements. The fabricated ablation probe encased in skin mimicking gel and return loss are shown in Figure 3.1. The measured return loss is in accordance with the simulation result, so these measurements suggest us to obtain liver and test the applicators in it. Figure 3.2 also shows S_{11} measurement result of the MW ablation probe in pig liver. As seen in both results, they provide a very large operation frequency range.

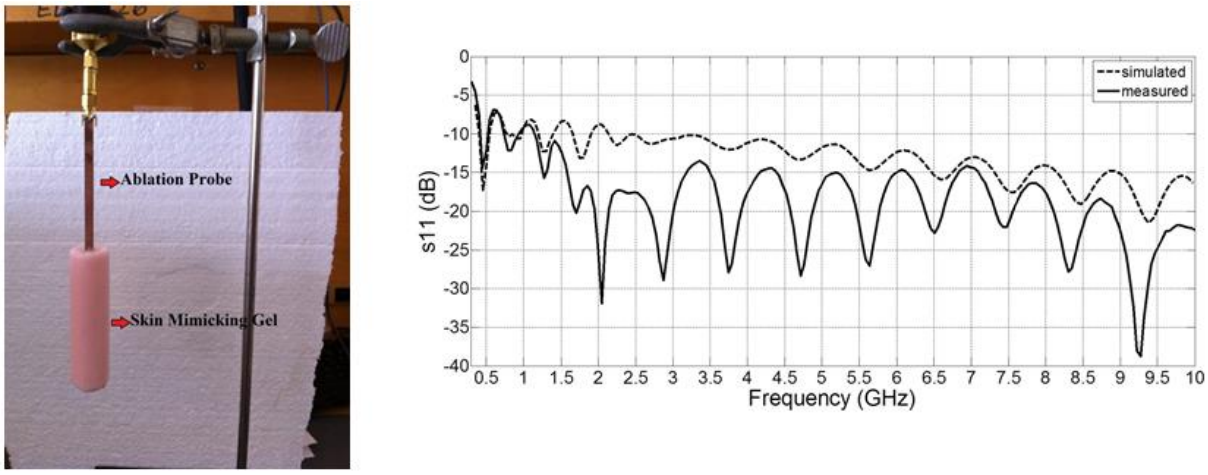

Figure 3.1 Fabricated MW ablation probe in skin mimicking gel for S_{11} measurement.

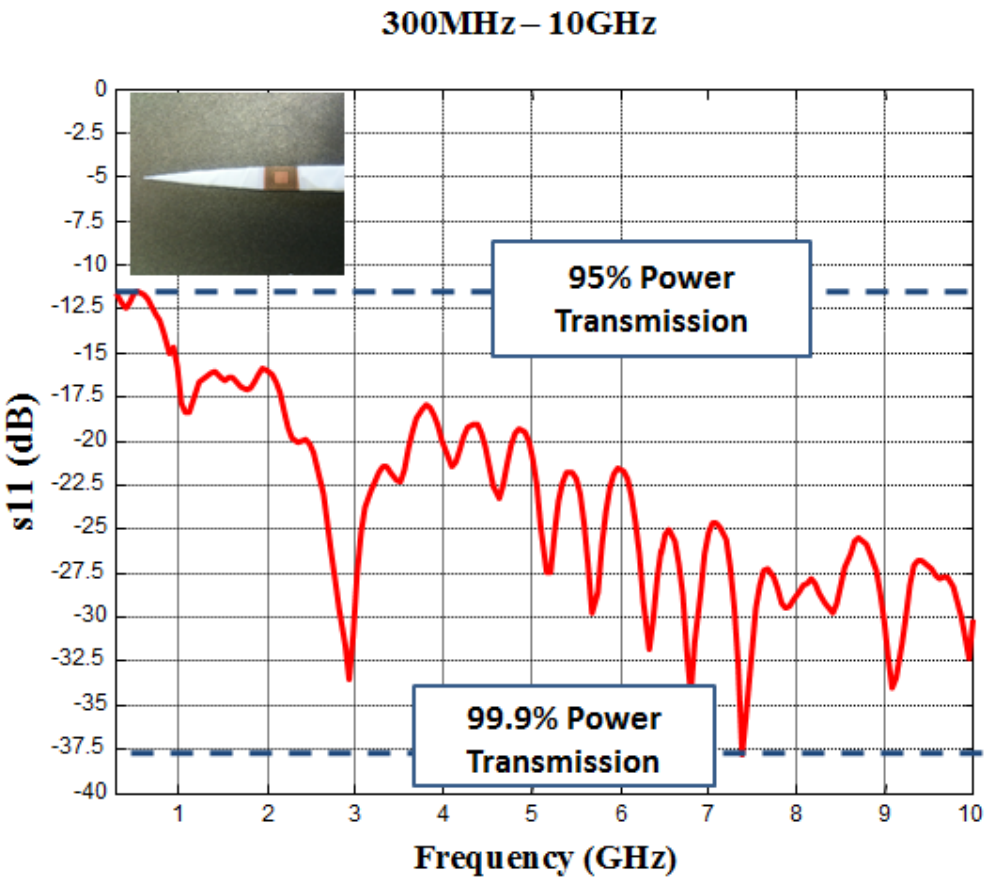

Figure 3.2 Antenna reflection from 300MHz to 10GHz in pig liver.

The experiment setup which includes signal generator, amplifier, ablation probes, fiber optic temperature sensors, pig liver and network analyzer is shown in Figure 3.3.

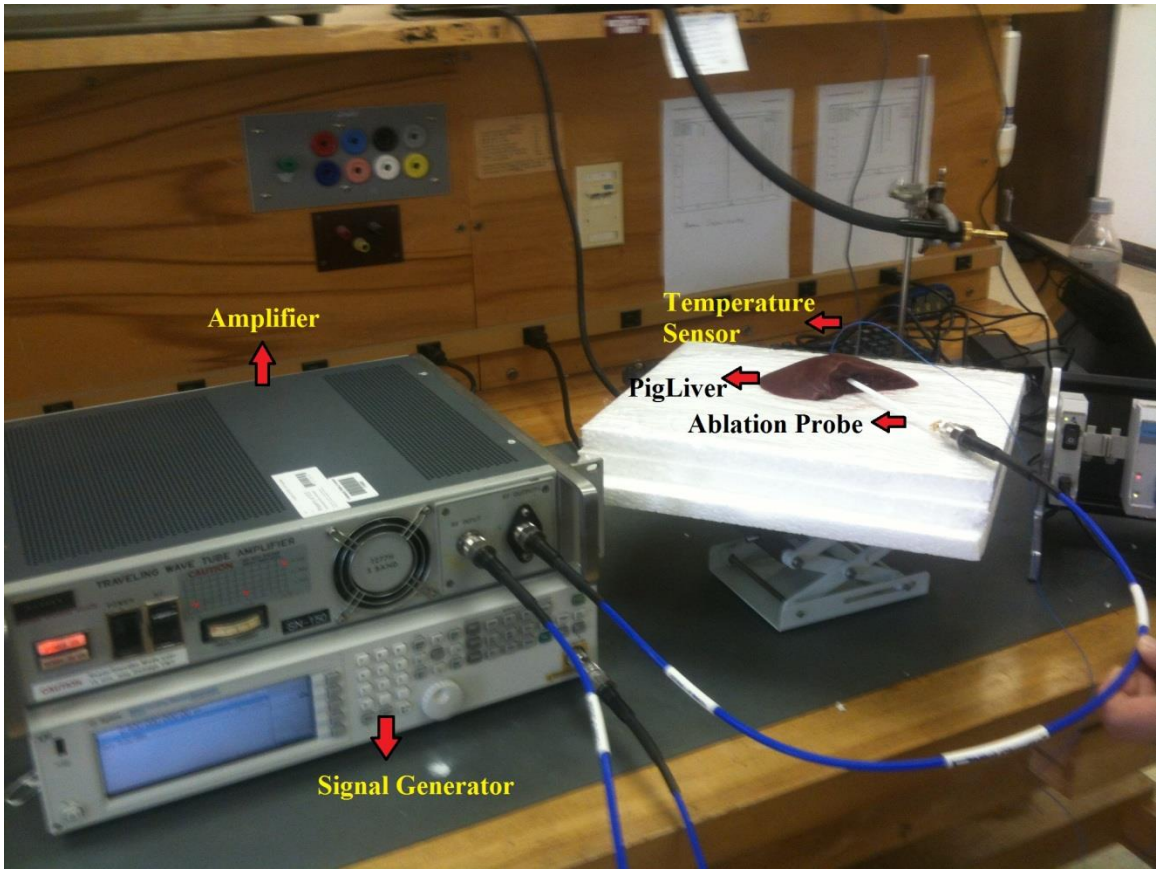

Figure 3.3 Experiment setup.

After probe placement inside the liver, the liver tissue is exposed to 20W at 2.4GHz for 4 minutes. The ablation zone of ex-vivo pig liver measurement at 2.4GHz is shown Figure 3.4.

Figure 3.4 Ablation zone in ex-vivo pig liver at 2.4 GHz.

Then, frequency of the signal is increased at 5.8GHz, and temperature is monitored by a fiber optic temperature sensor during the experiments. In Figure 3.5, preliminary results from ex-vivo pig liver experiments are shown at 5.8GHz.

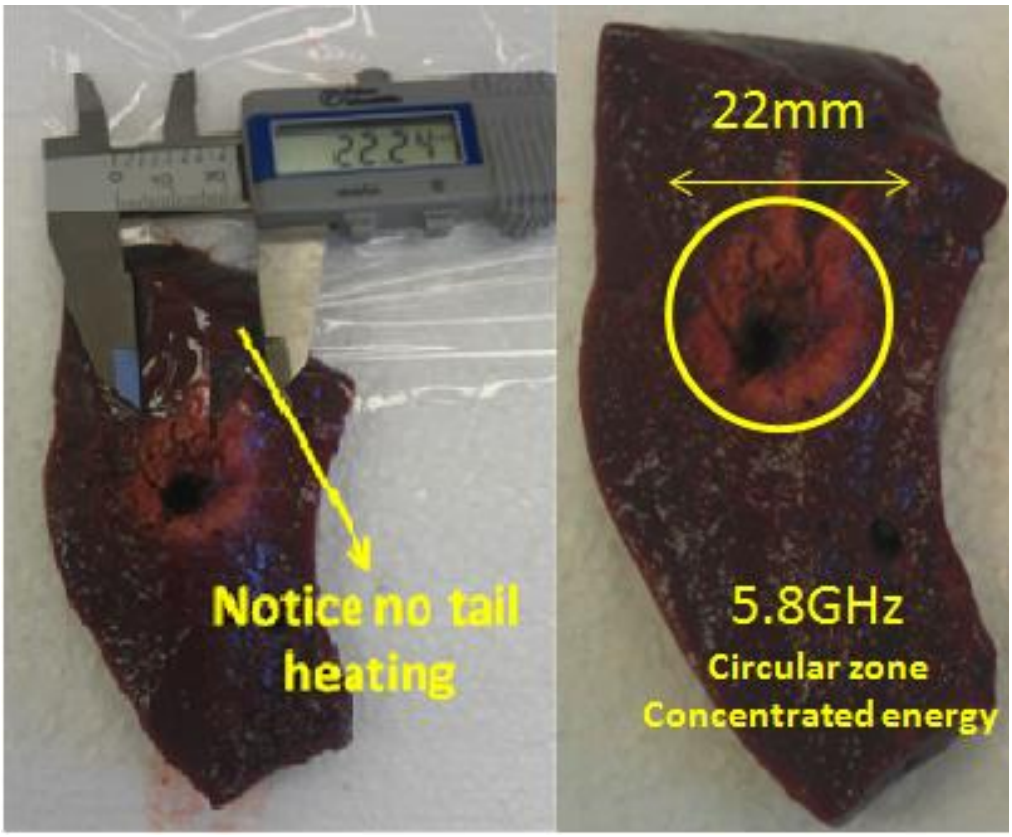

Figure 3.5 Ablation zone in ex-vivo pig liver at 5.8 GHz.

These measurements suggest that the ultra-wideband MW ablation applicator eliminates the unwanted ablation regions and allows increasing or decreasing ablation zones by adjusting the input frequency, as seen in Figure 3.4 and Figure 3.5. In addition, the power levels and ablation times are significantly lower than previously reported in literature. The results shown in the figures were generated using 20W input power with only 4 minutes of ablation. Also note that in Figure 3.5, we present the first ever MW ablation at 5.8 GHz, which is more circular and smaller than the zone at 2.4 GHz. It is envisioned that higher frequencies (5.8 GHz or higher) can be used for small tumors that

require smaller zones while lower frequencies (2.4 GHz, 915 MHz or lower) can be used for larger tumors.

As mentioned above, the first fabricated probe is tested in skin mimicking gel to verify the simulation results. After the verification, two more probes are fabricated, and fresh pig livers are taken from a local slaughter house. In order to keep the livers fresh, tests are done as soon as possible. If the livers wait for a while, the tissue can lose its actual properties, so it results in improper data.

At the beginning of the tests, a PNA network analyzer E8362B from Agilent is used for return loss measurement in skin mimicking gel and pig liver. An Agilent MXG analog signal generator is used to pump the signal through the amplifier. A Traveling Wave Tube Amplifier 1177H and 1277H from Hughes is used to amplify the signal coming from the signal generator for 5.8GHz and for 2,4GHz, respectively. As mentioned before, when a slot is excited with a suitable micro-strip excitation, it provides a large bandwidth. Figure 3.2 illustrates the reflection coefficient of the antenna when the probe is put in pig liver. Because of ultra-wideband nature of the resulting antenna, the power transmission efficiency is between 95% and 99.9% for all frequencies from 300 MHz to 10 GHz.

In actual studies, the MW antenna should be circularly wrapped around a probe. However, a cylindrical shaped antenna cannot be fabricated using our milling machine. A special catheter fabrication process needs to be pursued. In absence of fabrication, in order to show the potential of the conformal antenna applicator, we have performed simulations in HFSS. As a first step, a conformal antenna (applicator) that ensures antenna radiation at every single angle is drawn in HFSS, in order to demonstrate the

view of the future. The design and SAR simulation results are provided in Figure 3.6 and Figure 3.7, respectively.

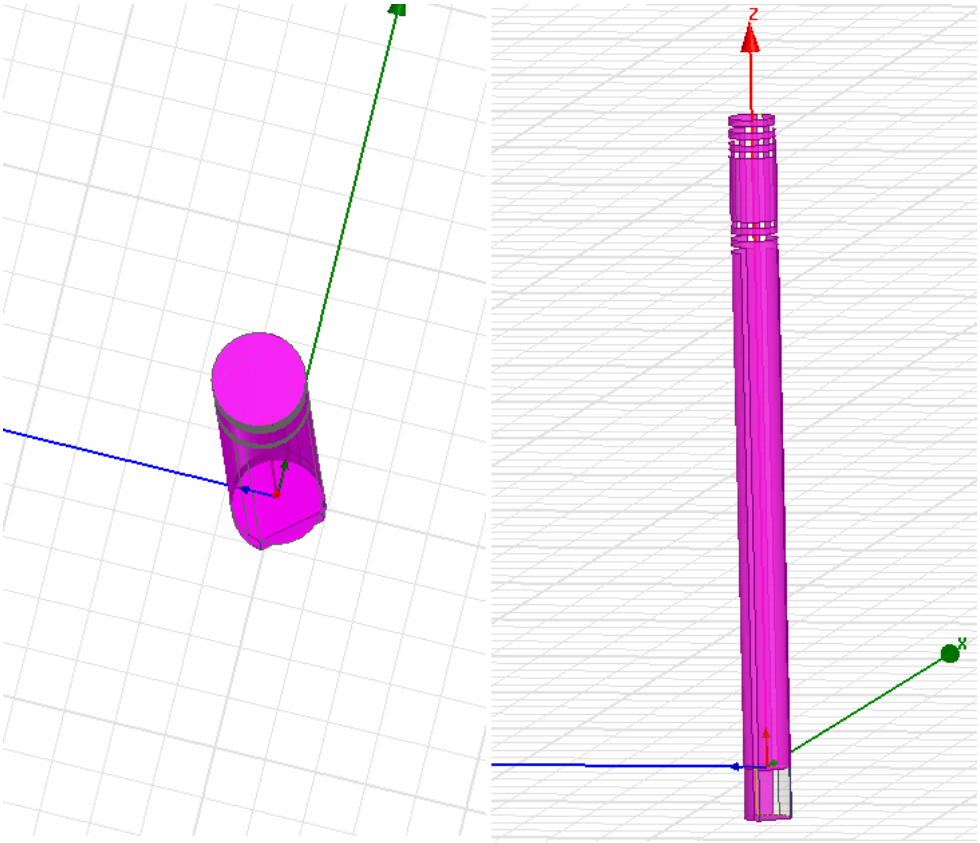

Figure 3.6 Cylindrical shaped ablation probe in HFSS.

SAR simulation is done to reveal the rate of the energy absorbed by the tissue and the uniform (360^{o}) energy radiation around the applicator representatively.

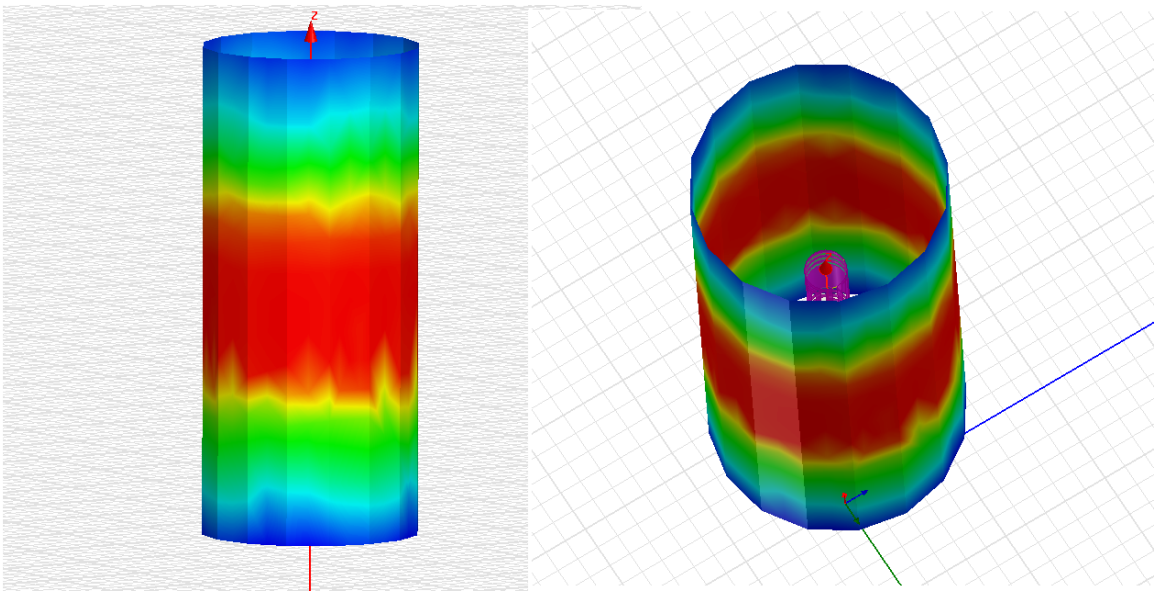

Figure 3.7 SAR results for cylindrical probe.

CHAPTER IV

CONCLUSION AND FUTURE WORK

In conclusion, an ultra-wideband microwave ablation applicator is designed and tested. The study shows that MW ablation can be applied using an ultra-wideband antenna. Also, during the tests, it was shown that different ablation zone sizes can be achieved by manipulating the frequency of applied signal. Therefore, single probe operations can be done instead of multiple probes operation to create larger ablation zone. Furthermore, this applicator reduces power requirements down to as low as 20W.

As a future work, these probes should be tested at lower frequencies in order to compare the ablation zones created by higher and lower frequencies. According to our experiments, lower frequencies (434 MHz, 608 MHz, and 915 MHz) can create larger ablation zones compared to 2.4 GHz and 5.8 GHz.

REFERENCES

[1] C. J. Simon, D. E. Dupuy, and W.W. Mayo-Smith, "Microwave ablation: principles and applications," *RadioGraphics*, pp. 69-83, Oct. 2005.

[2] I. D. McRury and D. E. Haines, "Ablation for the treatment of arrhythmias," *Proc. IEEE*, vol.84, no.3, March 1996.

[3] T. L. Wonnell, P. R. Satuffer, and J. J. Langberg, "Evaluation of microwave and radio frequency catheter in myocardium-equivalent phantom model," *IEEE Trans. Biomed. Eng.*, vol.39, no.10, Oct. 1992.

[4] T. Seki et al., "Ultrasonically guided percutaneous microwave coagulation therapy for small hepatocellular carcinoma," *Am. J. Gastroenterol.*, vol.74, pp. 817-825, Aug. 1994.

[5] T. Matsukawa et al., "Percutaneous microwave coagulation therapy in liver tumors: a 3-year experience," *Acta Radiologica*, vol.38, pp. 410-415, May 1997.

[6] W.S. Halsted, "The result of operations for the cure of cancer of the breast performed at Johns Hopkins Hospital from June, 1889, to January, 1894," *Ann. Surg.*, vol.20, pp.497-555, Nov. 1894.

[7] M. E. Ulucakli, Y. Subedi, and I. –C. Ang, "Radiofrequency ablation of tumors," *Proc. IEEE 31st Ann. Northeast Bioengineering Conf.*, 2005, pp. 94-95.

[8] G. Carrafiello et al., "Microwave tumors ablation: principles, clinical applications and review of preliminary experiences," *Int. J Surg.*, vol.6, pp.65-69, Jan.2009.

[9] E. S. Glazer and S. A. Curley, "the ongoing history of thermal therapy for cancer," *Surg. Oncol. Clin. N. Am.*, vol. 20, pp. 229-235, Apr. 2011.

[10] Y. Minami and M. Kudo, "Radiofrequency ablation of hepatocellular carcinoma: a literature review," *Int. J. Hepatol.*, vol. 2011, pp. 1-9, Feb. 2011.

[11] Y. K. Cho, J. K. Kim, W. T. Kim, and J. W. Chung, "Hepatic resection versus radiofrequency ablation for very early stage hepatocellular carcinoma: a markov model analysis," *Hepatology*, vol. 51, no. 4, pp. 1284–1290, Apr. 2010.

[12] S. Mulier et al., "Radiofrequency ablation versus resection for resectable colorectal liver metastases: time for a randomized trial? an update," *Dig. Surg.*, vol. 25, no. 6, pp. 445–460, 2008.

[13] K. K. Ng et al., "Thermal ablative therapy for malignant liver tumors: a critical appraisal," *J Gastroenterol Hepatol.*, vol.18, pp. 616-629, June 2003.

[14] B. Rubinsky, "Cryosurgery," *Annu Rev Biomed Eng.*, vol. 2, pp. 157- 187, Aug. 2000.

[15] R. W. Habash, R. Bansal, D. Krewski, and H. T. Alhafid, "Thermal therapy, part iii: ablation techniques," *Crit. Rev. Biomed. Eng.*, vol. 35, pp. 37-121, 2007.

[16] D. E. Haines, "Thermal ablation of perfused porcine left ventricle in vitro with the neodymium-YAG laser hot tip catheter system," *Pacing Clin. Electrophysiol.*, vol.15, pp. 979-985, Aug. 1992.

[17] J. Langberg et al., "Catheter ablation of accessory pathways using radiofrequency energy in the canine coronary sinus," *J. Am. Coll. Cardiol.*, vol.13, pp. 491-496, Feb. 1989.

[18] J. Langberg et al., "Catheter ablation of the atrioventricular junction with radiofrequency energy," *Circulation*, vol.80, pp. 1527-1535, Dec. 1989.

[19] A. E. Sperstein, S. J. Rogers, P. D. Hansen, and A. Gitomirsky, "Laparoscopic thermal ablation of hepatic neuroendocrine tumor metastases," *Surgery*, vol. 122, pp. 1147-1155, Dec. 1997.

[20] R. Lencioni et al., "Radio-frequency thermal ablation of liver metastases with cooled-tip electrode needle: results of a pilot clinical trial," *Eur. Radiol.,* vol. 8, pp. 1205-1211, 1998.

[21] S. A. Curley et al., "Radiofrequency ablation of unresectable primary and metastatic hepatic malignancies: results in 123 patients," *Ann. Surg.*, vol. 230, pp. 1-8, Jul. 1999.

[22] M. Friedman et al., "Radiofrequency ablation of cancer," *J. Cardiovasc. Intervent. Radiol.*, vol.27, pp. 427-434, June 2004.

[23] S. Pisa, M. Cavagnaro, P. Bernardi, and J. C Lin, "A 915-MHz antenna for microwave thermal ablation treatment: physical design, computer modeling and experimental measurement," *IEEE Trans. Biomed. Eng.*, vol. 48, no. 5, pp., 599-601, May 2001.

[24] C. L. Brace, "Radiofrequency and microwave ablation of the liver, lung, kidney and bone: what are the differences?" *Curr. Probl. Diagn. Radiol.*, vol.38, pp. 135-143, May 2009.

[25] M. R. Williams, M. Garrido, M. C. Oz, and M. Argenziano, "Alternative energy sources for surgical atrial ablation," *J Card. Surg.*, vol. 19, pp. 201-206, May 2004.

[26] "Diagram of RFA procedure," [online]. Available: http://www.upmc.com/services/liver-cancer/treatments/radiofrequency/pages/rfa-images.aspx

[27] L. T. Blouin and F. I. Marcus, "The effect of electrode design on the efficiency of delivery of radiofrequency energy to cardiac tissue in vitro," *Pacing Clin. Electrophysiol.*, vol.12, pp. 136-143, Jan. 1989.

[28] F. H. Wittkampf, R. N. Hauer, and E. O. Robles de Medina, "Control of radiofrequency lesion size by power regulation," *Circulation*, vol.80, pp. 962-968, Oct. 1989.

[29] R. D. Nevels, G. D. Arndt, G. W. Raffoul, J. R. Carl, and A. Pacifico, "A microwave catheter design," *IEEE Trans. Biomed. Eng.*, vol.45, pp. 885-890, Jul. 1998.

[30] A. Goette, S. Reek, H. U. Klein, and J. C. Geller, "Case report: severe skin burn at the site of the indifferent electrode after radiofrequency catheter ablation of typical atrial flutter," *J. Interv. Card. Electrophysiol.*, vol.5, pp. 337-340, Sep. 2001.

[31] C. J. Simon et al., "Intraoperative triple antenna hepatic microwave ablation," *Am. J. Roentgenol.*, vol.187, pp. 333-340, Oct. 2006.

[32] D. M. Lloyd et al., "International multicenter prospective study on microwave ablation of liver tumours: preliminary results," *HPB (Oxford)*, vol.13, pp. 579-585, Aug. 2011.

[33] "UC San Diego first hospital in region to offer microwave technology to destroy liver tumors," [online]. Available: http://www.universityofcalifornia.edu/news/article/19450

[34] M. G. Lubner, C. L. Brace, J. L. Hinshaw, and F. T. Jr. Lee, "Microwave tumor ablation: mechanism of action, clinical results, and devices," *J. Vasc. Interv. Radiol.,* vol.21, pp. 192-203, Aug. 2010.

[35] P. Liang and Y. Wang, "Microwave ablation of hepatocellular carcinoma," *Oncology*, vol. 72, pp. 124-131, Dec. 2007.

[36] D. Yang, M. C. Converse, D. M Mahvi, and J. G. Webster, "Measurement and analysis of tissue temperature during microwave liver ablation," *IEEE Trans. Biomed. Eng.*, vol. 54, pp. 150-155, Jan. 2007.

[37] M. M. Awad, L. Devgan, I. R. Kamel, M. Torbensen, and M. A. Choti, "Microwave ablation in a hepatic porcine model: correlation of CT and histopahologic findings," *HPB (Oxford)*, vol. 9, pp. 357-362, 2007.

[38] B. B. Vander et al., "Microwave ablation using a wide-aperture antenna design in a porcine thigh muscle preparation: in vivo assessment of temperature profile and geometry," *J. Cardiovasc. Electrophysiol.*, vol.11, pp. 193-198, 2000.

[39] "IEEE standard definitions of terms for antennas," [online]. Available: http://ieeexplore.ieee.org/stamp/stamp.jsp?tp=&arnumber=30651

[40] "Antenna field regions," [online]. Available: http://www.ece.msstate.edu/~donohoe/ece4990notes2.pdf

[41] P. S. Nakar, "Design of a compact microstrip patch antenna for use in wireless/cellular devices," M.S. thesis, Dept. Elect. Comp. Eng. Florida State Univ., Tallahassee, FL, 2004.

[42] C.A. Balanis, *Antenna Theory: Analysis and Design*, New York, NY: John Wiley & Sons, 1997.

[43] "Dielectric Properties of Body Tissues," [Online]. Available: http://niremf.ifac.cnr.it/tissprop

[44] E. Topsakal, "Antennas for medical applications: ongoing research and future challenges," in *International Conference on Electromagnetics in Advanced Applications*, 2009, pp. 890-893.

[45] T. Yilmaz, T. Karacolak, and E. Topsakal, "Characterization and Testing of a Skin Mimicking Material for Implantable Antennas Operating at ISM Band (2.4 GHz–2.48 GHz)," *IEEE Antennas Wireless Propag. Lett.*, vol. 7, pp. 418-420, June 2008.